

Fig S1 A population of kinetochores can be found at a distance from SPBs in Noc-treated *CDC15* and *cdc15-2* cells. (A) CEN V-RFP can be found at a distance from Ndc80p-GFP in Noc-arrested cells. Cells carrying *cdc20::pMET-CDC20 NDC80-GFP CEN V-RFP* in *CDC15* (i) and *cdc15-2* (ii) backgrounds were arrested in metaphase by *cdc20*-depletion at 32°C (a). The *CEN5::tetO2X112* located 1.4kb left of *CEN V* (Tanaka et al., 2000) together with the *tetR-RFP* served as a marker for the localization of kinetochore on chromosome V and allowed us to examine the relative position of a specific kinetochore in relation to the rest of the kinetochores marked by Ndc80p-GFP. In parallel experiments, the strains were arrested in Noc 32°C (b). There appeared to be no significant difference in the percentages of cells with such kinetochores losing association in *CDC15* and *cdc15-2* cells. (B) Ndc80p-GFP can be found at a distance from Spc29p-RFP in Noc-arrested cells. Cells carrying *cdc20Δ GAL-CDC20 NDC80-GFP SPC29-RFP* in *CDC15* (i) and *cdc15-2* (ii) backgrounds were arrested in metaphase by *cdc20*-depletion at 32°C (a). In parallel experiments, the strains were arrested in Noc 32°C (b). Both the *CDC15* and *cdc15-2* strains showed that a small population of the cells exhibited weak Ncd80p-GFP signals at a distance from the Spc29p-RFP (Noc, bottom panels, and magnified regions with white arrows). This was consistent with data from a previous report (Gillett et al., 2004). (C) CEN V-GFP can be found at a distance from Spc29p-RFP in Noc-arrested cells. *cdc20Δ::GAL-CDC20 CEN V-GFP SPC29-RFP* in *CDC15* (i) and *cdc15-2* (ii) backgrounds arrested in metaphase by *cdc20*-depletion at 32°C (a). In parallel experiments, the strains were arrested in Noc 32°C (b). Similar percentages of *CDC15* and *cdc15-2* cells were found to display CEN V-GFP signals at a distance away from the Spc29p-RFP. All images were taken at the arrested stage using spinning disk confocal microscopy.

Fig S2 CEN V-GFP drifts away from SPBs in some Noc-treated cells. Wild-type *tetR-GFP CEN5::tetO2X112 SPC29-RFP MYO1-Redstar2* cells were treated in alpha-factor and then released into Noc-containing media on slides for time-lapsed imaging. (A) In most cells, the CEN V-GFP spots were closely-associated with Spc29p-RFP (i). The tracking of Spc29p-RFP and CEN V-GFP as indicated by the pathways taken by them (ii) suggested that the SPBs and CEN V undergo dynamic movements. (B) In some cells maintained in Noc-containing media, the CEN V-GFP spots were found to move away from Spc29p-RFP (i). The tracking of lines Spc29p-RFP and CEN V-GFP are shown in (ii).

Fig S3 Time-lapsed imaging of Mad2p-GFP in wild-type (i) and *cdc15-2* cells (ii) released from Noc arrest to YPD at 32°C as described in Fig 4. (iii) Graph shows the percentages of wild-type and *cdc15-2* cells with persistent Mad2p-GFP signals after Ndc80p-Redstar2 has separated.

Fig S4 Time-lapsed images showing *cdc20Δ GAL-CDC20 CEN V-GFP SPC29-RFP* released from *Cdc20p*-depletion into YPD at 32°C. CEN V-GFP and Spc29p-RFP do not show oscillation through the neck as the cell separated Spc29p-RFP and CEN V-GFP.

Fig S5 Biorientation of CEN V-GFP spots is normal in *cdc20*-arrest in *cdc15-2* cells. *cdc20Δ GAL-CDC20 CEN V-GFP SPC29-RFP* (A) and *cdc15-2 cdc20Δ GAL-CDC20 CEN V-GFP SPC29-RFP* (B) cells were arrested in YPD for 2.5 hrs at 24°C and YPD for 2.5 hrs at 32°C before being transferred into SC/Glu and imaged on the heated-stage. (C) Cell counts showing percentage of cells with biorientated CEN V-GFP. (D) and (E) close-up images of CEN V-GFP in *CDC15* and *cdc15-2* cells reveal longer distances between Spc29p-RFP in *cdc15-2* cells. (F)

Plots show the distance between Spc29p-RFP in 106 cells for each strain in the experiment as described in (A) and (B). In parallel experiments, *cdc20Δ GAL-CDC20 CEN V-GFP SPC29-RFP PDS1-HA* and *cdc15-2 cdc20Δ GAL-CDC20 CEN V-GFP SPC29-RFP PDS1-HA* cells were arrested as described in (A) and (B) and Western blot analysis performed on lysates obtained at the Cdc20p-depleted stage to determine Pds1p and Pgk1p levels.

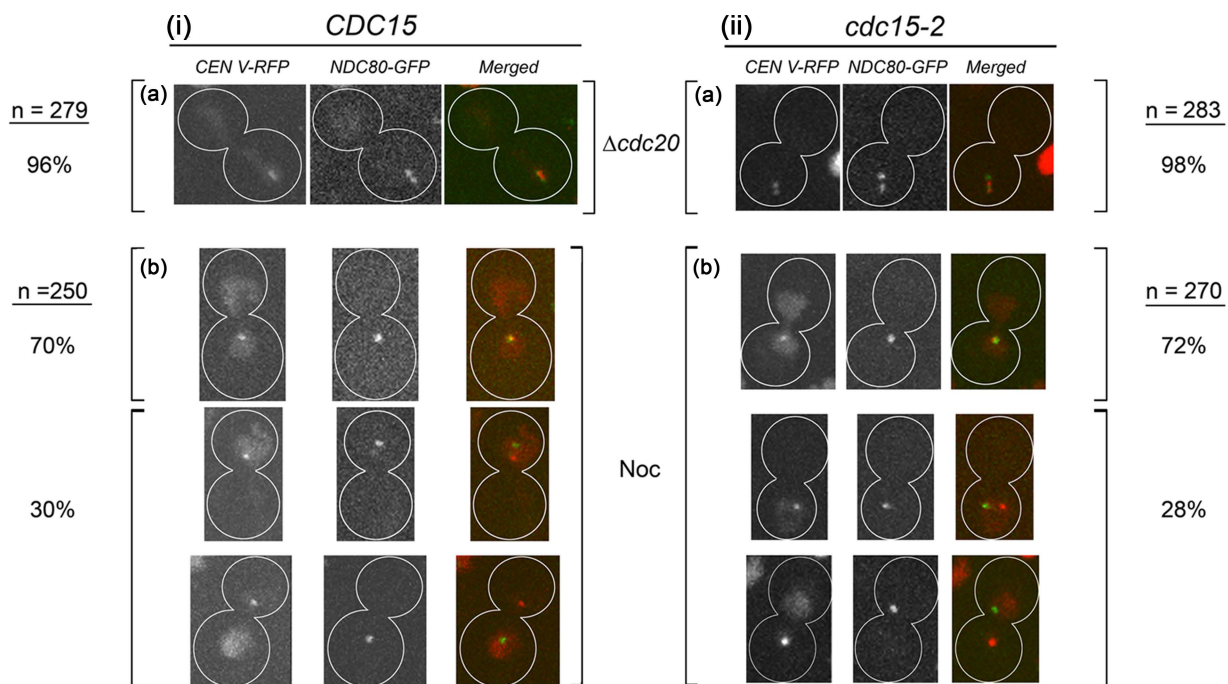
Fig S6 Ipl1p and Sli15p localized to *cdc15-2* cells similarly as in wild-type cells. Wild-type (i) and mutant (ii) cells carrying *IPL1-GFP MYO1-REDSTAR2* (A) and *SLI15-GFP MYO1-REDSTAR2* (B) were treated as in Fig 4.

Fig S7 Flow-chart showing the regime for the experiment performed as described in Fig 7.

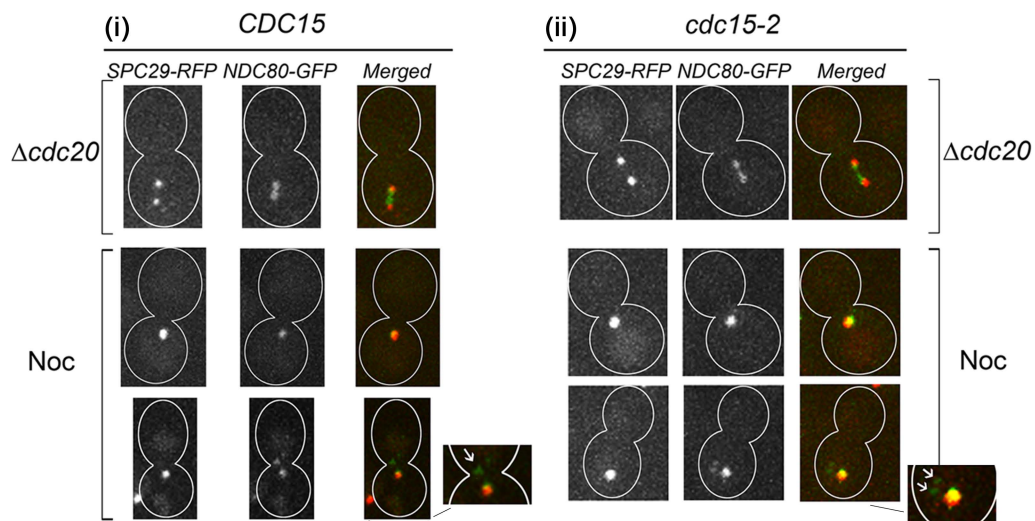
Movie 1 Dynamic movement of Spc29p-RFP across the neck in relation to CEN V-GFP and Myo1p-Redstar2 in wild-type cell. The movie shown is of the cell described in Fig 4Ai.

Movie 2 Dynamic movement of Spc29p-RFP across the neck in relation to CEN V-GFP and Myo1p-Redstar2 in *cdc15-2* cell. The movie shown is of the cell described in Fig 4Aii.

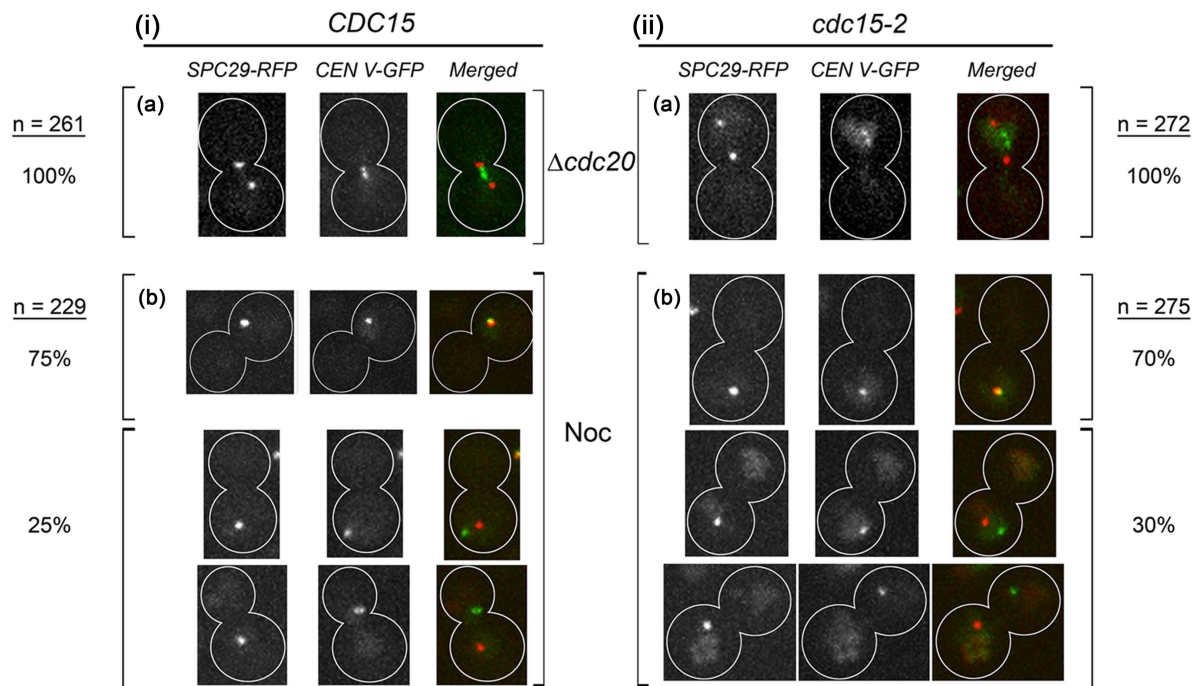
A

cdc20::pMET-CDC20 NDC80-GFP CEN V-RFP

B

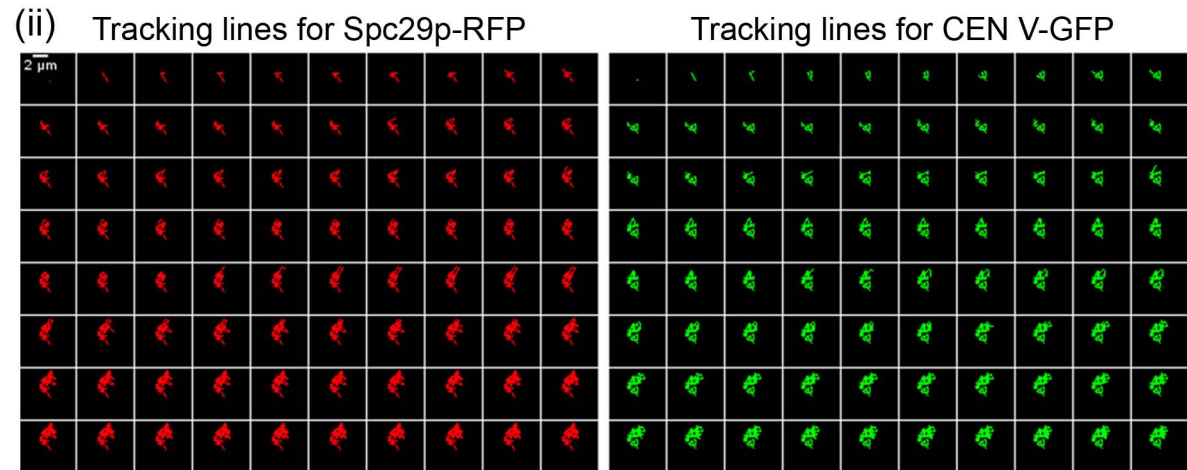
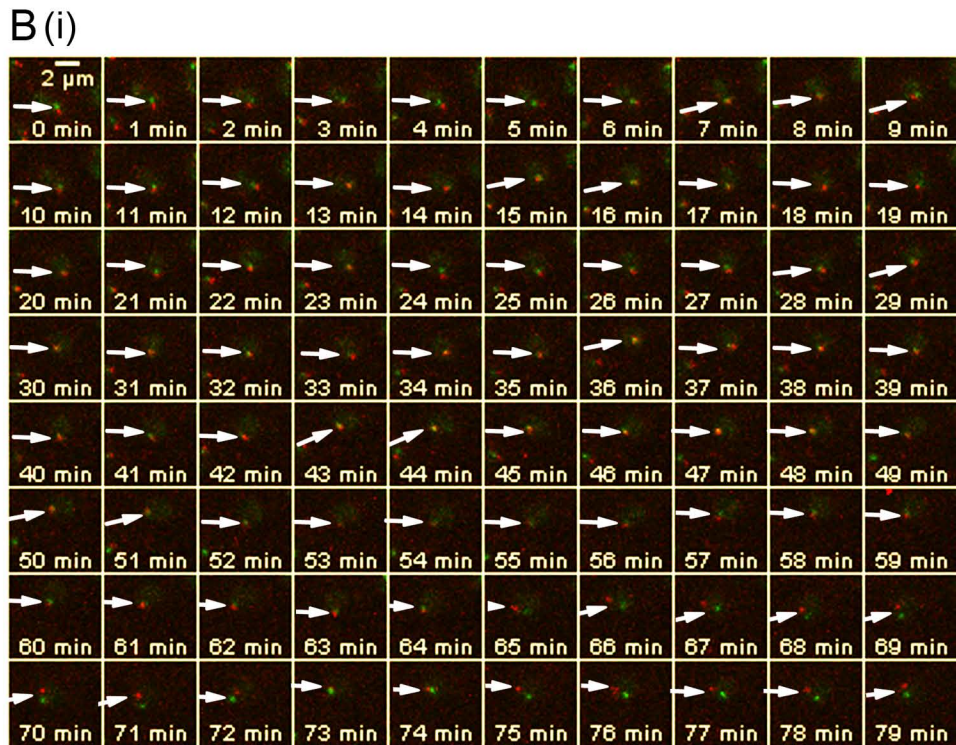
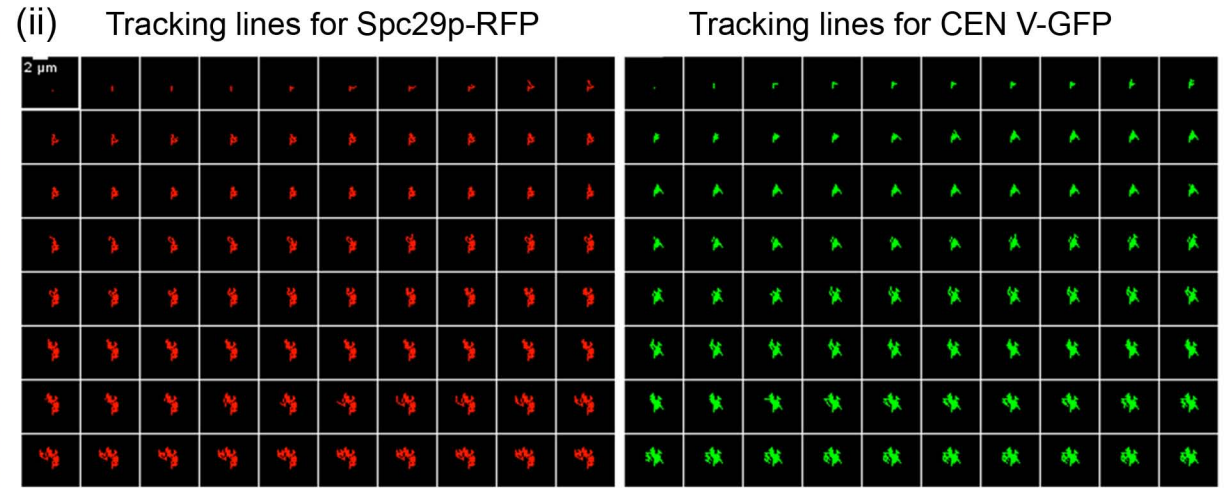
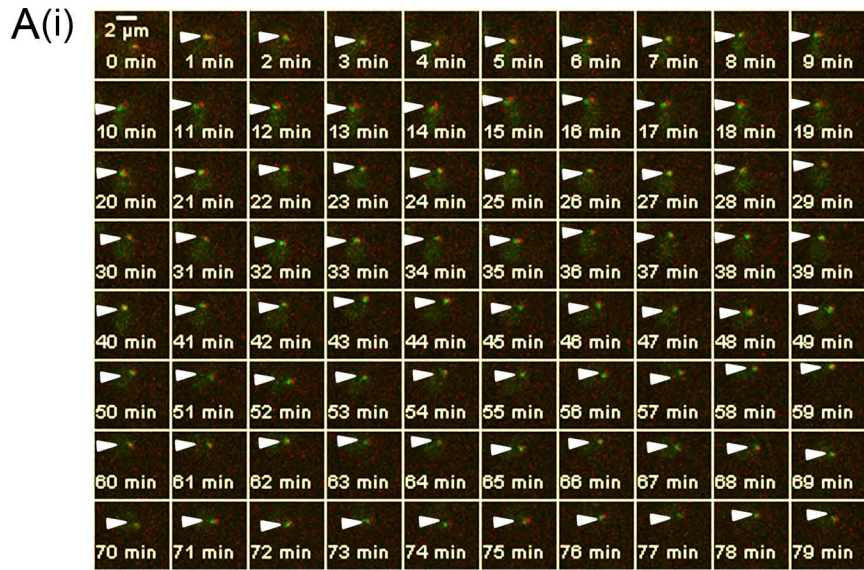
cdc20 Δ GAL-CDC20 NDC80-GFP SPC29-RFP

C

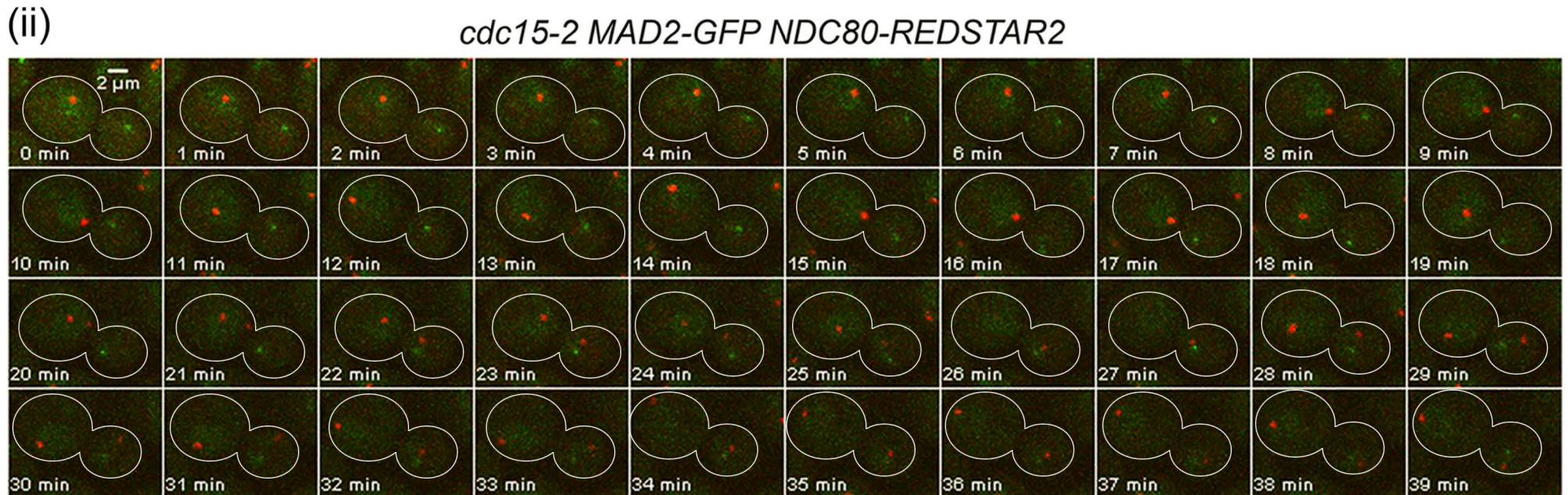
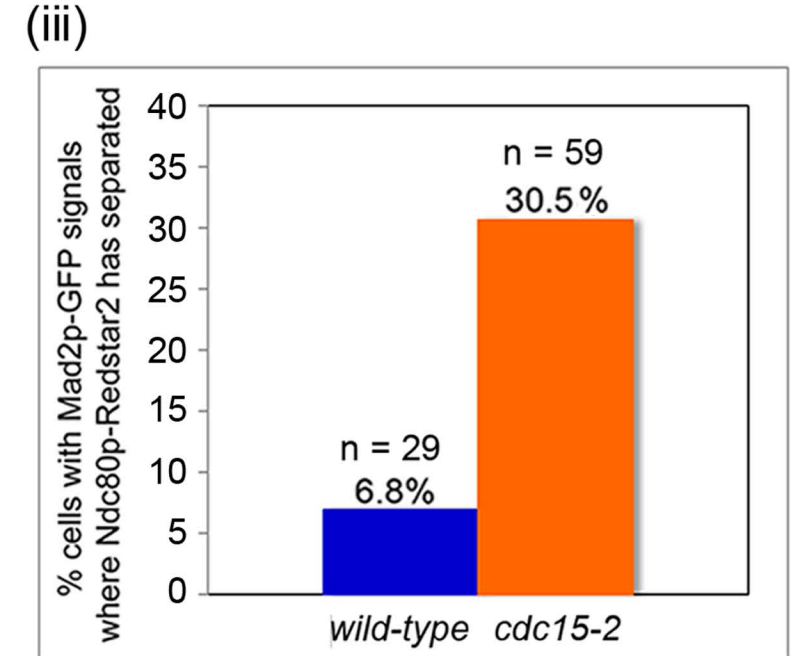
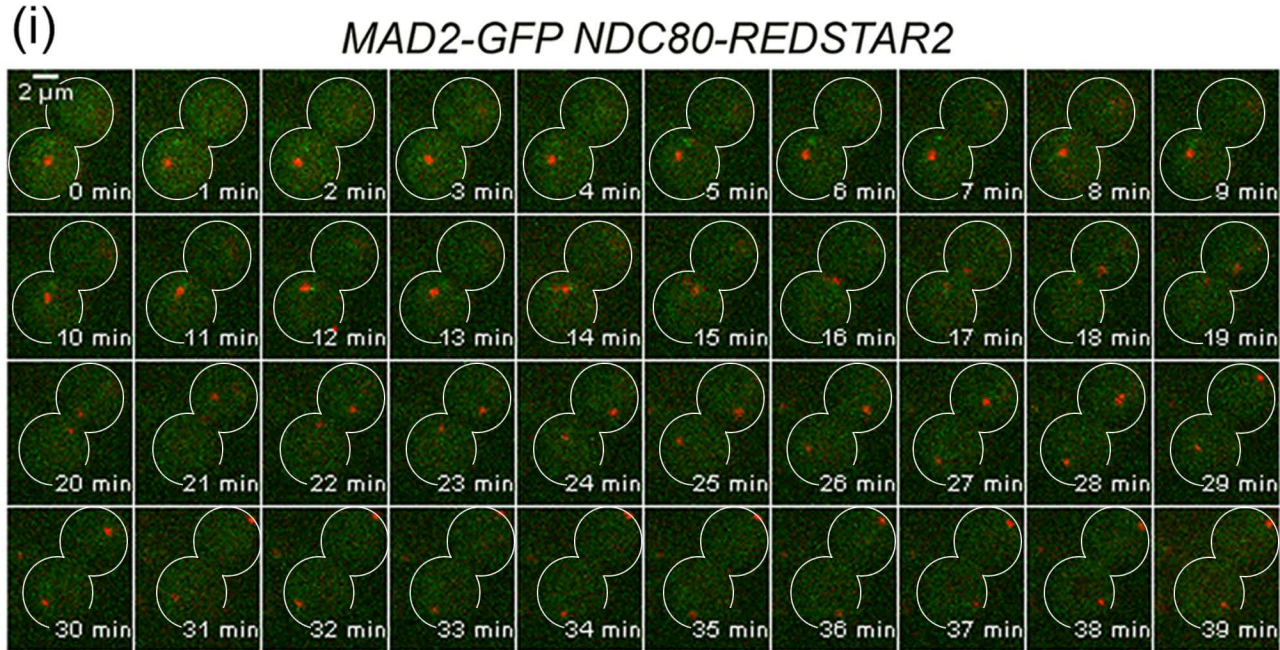
cdc20 Δ GAL-CDC20 CEN V-GFP SPC29-RFP

CEN V-GFP SPC29-RFP MYO1-REDSTAR2

α F arrest \longrightarrow release into YPD + Noc for 1 min \longrightarrow SC/Glu + Noc on slide for time-lapsed imaging

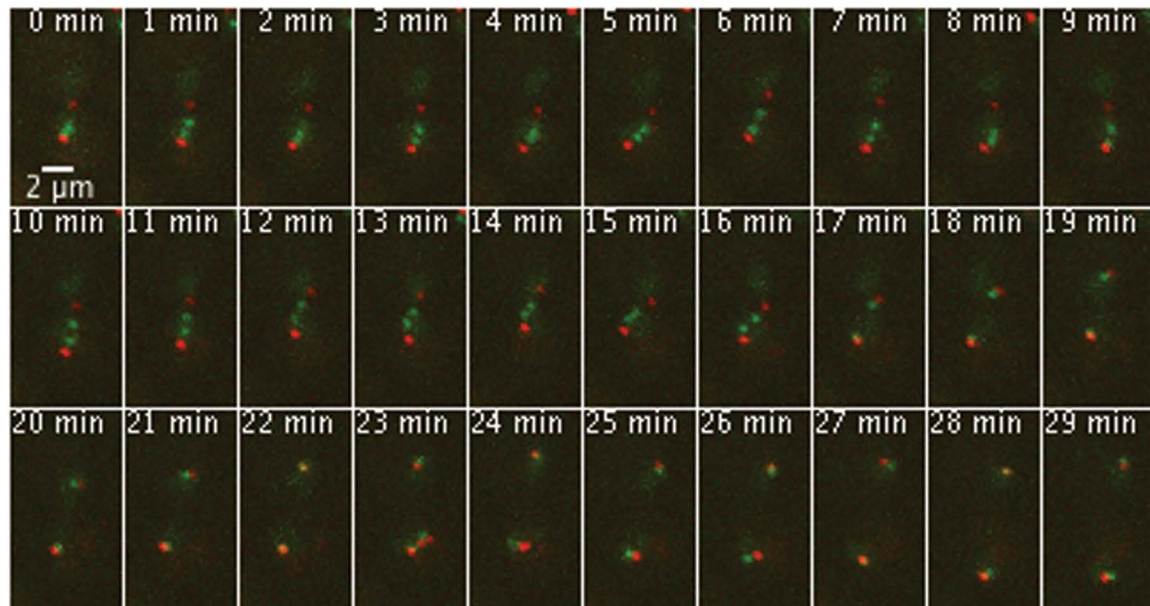


YPD + Noc, 24°C -> YPD + Noc, 32°C -> SC/Glu, 32°C (time-lapsed)

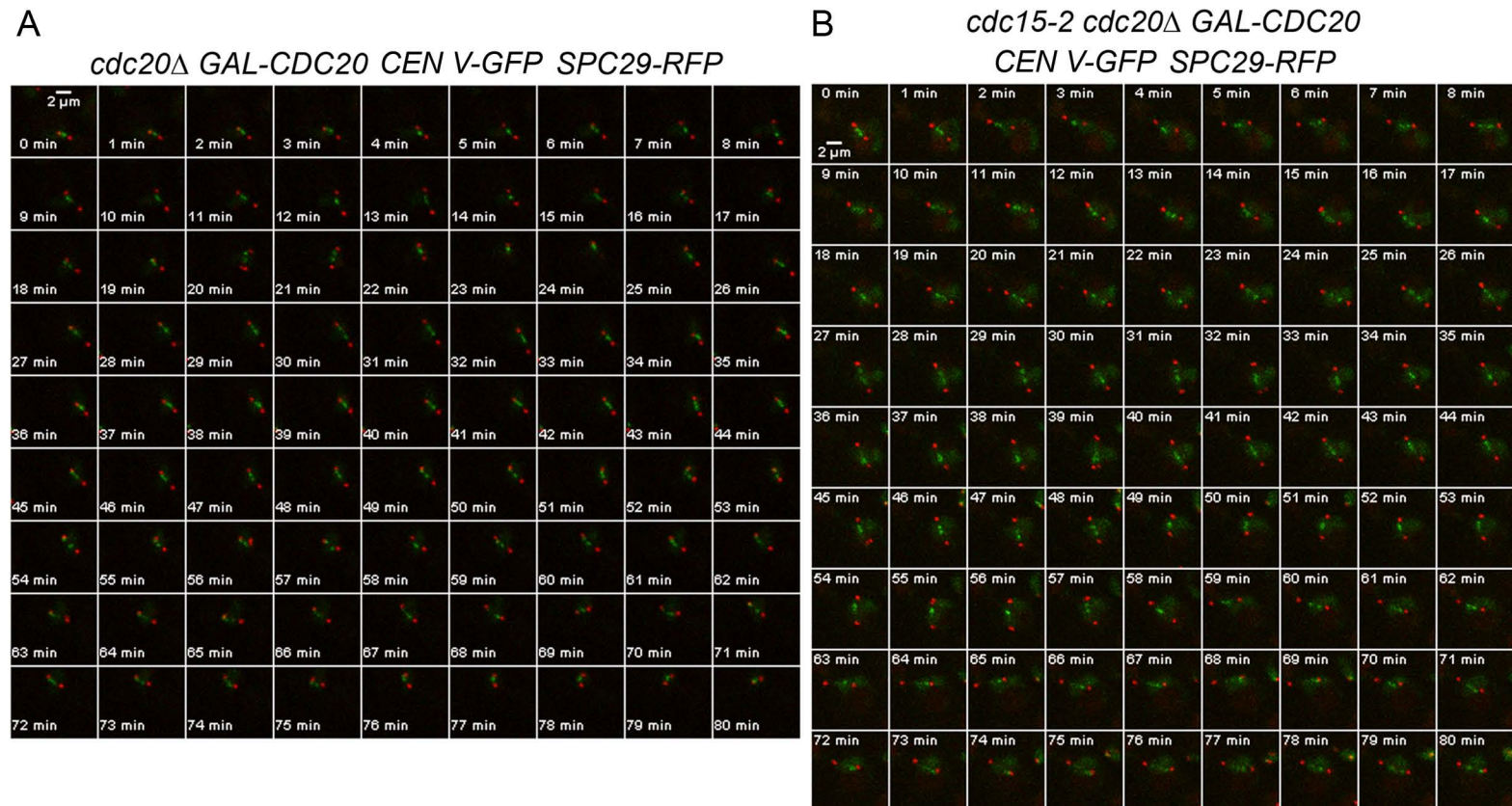


YPD arrest → release into YP/Raff/Gal
(cdc20-depletion)

*cdc20*Δ GAL-CDC20 CEN V-GFP SPC29-RFP

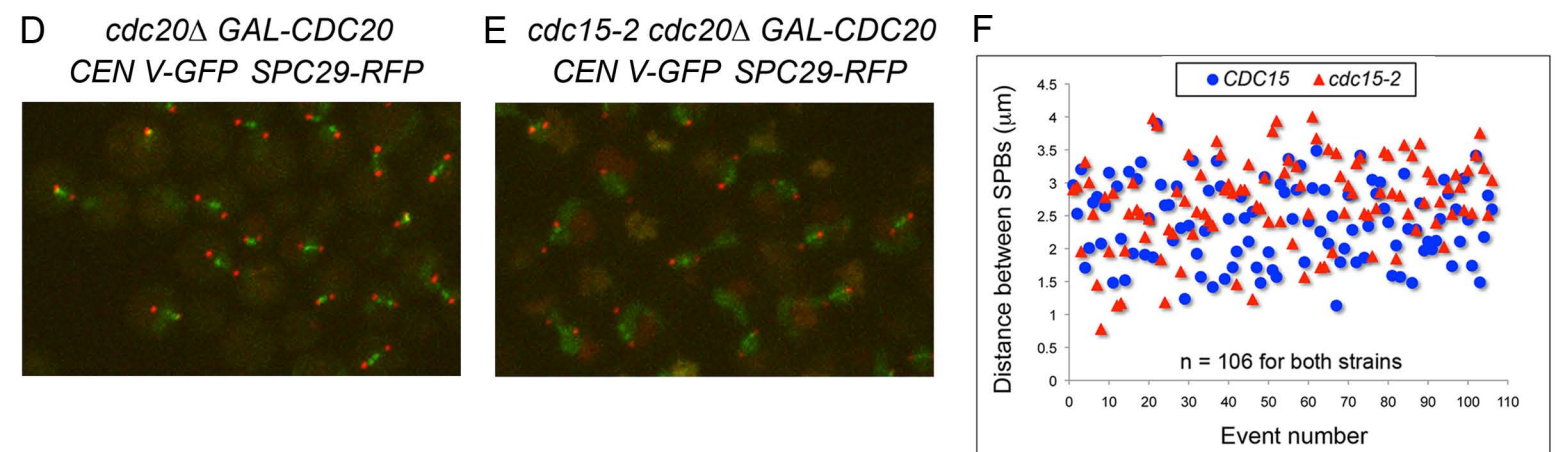


YPD, 24°C -> YPD, 32°C -> SC/Glu, 32°C



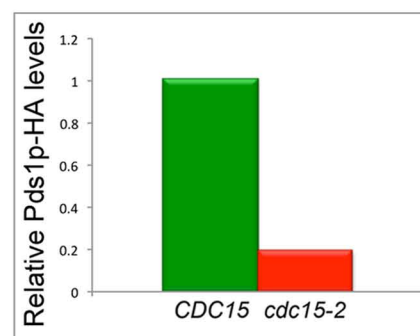
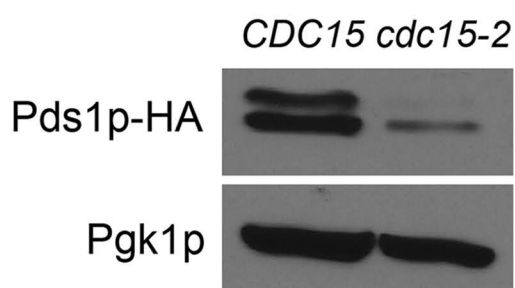
C

Strain background	% cells showing biorientation of CEN V-GFP spots
<i>CDC15</i> (n = 49)	100
<i>cdc15-2</i> (n = 44)	97.7



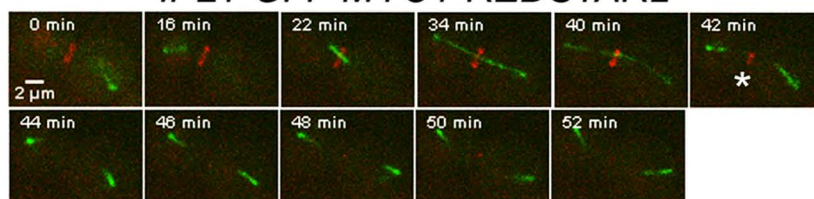
G YPD, 24°C -> YPD, 32°C

cdc20Δ GAL-CDC20 CEN V-GFP SPC29-RFP PDS1-HA

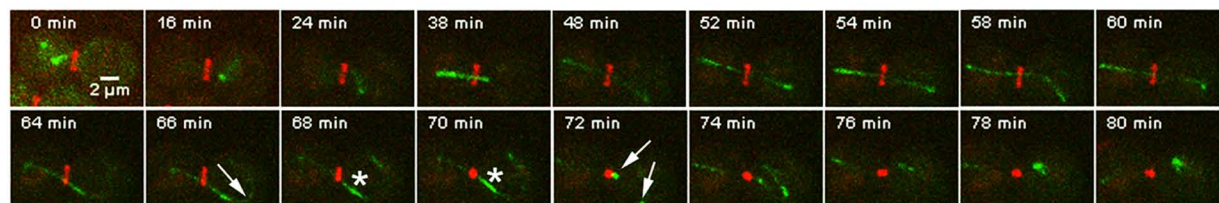


A

(i)

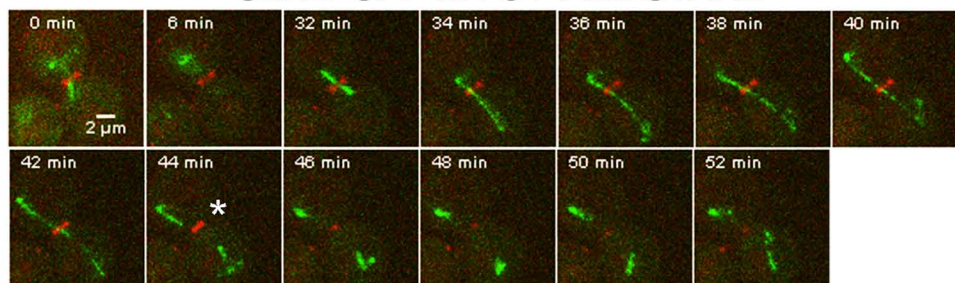
IPL1-GFP MYO1-REDSTAR2

(ii)

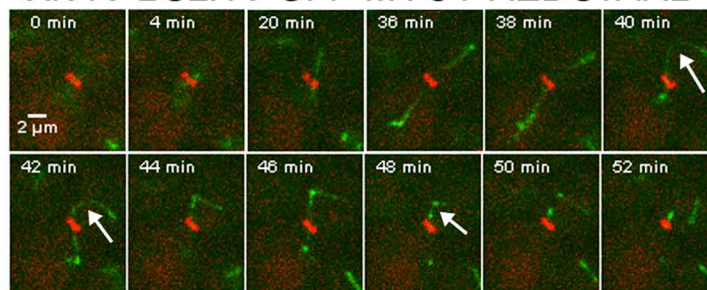
cdc15-2 IPL1-GFP MYO1-REDSTAR2

B

(i)

SLI15-GFP MYO1-REDSTAR2

(ii)

cdc15-2 SLI15-GFP MYO1-REDSTAR2

cdc15-2 pMET-PDS1-myc CEN V-GFP SP29-RFP MYO1-Redstar2

